

Double Anomalous Peak in the Heat Capacity Just Below the Triple Point of Saturated $e\text{-H}_2$ with $\text{FeO}(\text{OH})^1$

T. Nakano,^{2,3} W. L. Tew,⁴ O. Tamura,² and H. Sakurai²

The heat capacity of $e\text{-H}_2$ with powder of $\text{FeO}(\text{OH})$ used as a catalyst for ortho-para equilibration has been investigated using sealed cells fabricated at the National Institute of Standards and Technology and at the National Metrology Institute of Japan. An anomalous double peak has been observed in their heat capacities at temperatures just below the triple point independent of sources of H_2 and $\text{FeO}(\text{OH})$ and designs of sealed cells. Supercooling behavior has been observed not only at the triple point but also at each anomalous peak resulting from a depression of the melting temperature of a portion of solid H_2 in close physical proximity to the catalyst. The reduction of the amount of catalyst suppresses the size of the anomalies and allows one to obtain more reliable melting curves for $e\text{-H}_2$ at the triple point.

KEY WORDS: catalyst; $\text{FeO}(\text{OH})$; hydrogen; ITS-90; triple point.

1. INTRODUCTION

The triple point of spin-equilibrated molecular hydrogen ($e\text{-H}_2$) at 13.8033 K is one of the defining fixed points of the International Temperature Scale 1990 (ITS-90) and is used to calibrate standard platinum resistance thermometers and interpolation gas thermometers [1]. A large amount

¹Paper presented at the Fifteenth Symposium on Thermophysical Properties, June 22–27, 2003, Boulder, Colorado, U.S.A.

²National Metrology Institute of Japan, AIST Central 3, Tsukuba, Ibaraki 305-8563, Japan.

³To whom correspondence should be addressed. E-mail: tnt@ni.aist.go.jp

⁴Process Measurements Division, National Institute of Standards and Technology, 100 Bureau Drive, Stop 8363, Gaithersburg, Maryland 20899-8363, U.S.A.

of powder of a catalyst (such as ferric oxy-hydroxide ($\text{FeO}(\text{OH})$) is traditionally used to establish the equilibrium concentration of two isomers of molecular hydrogen (H_2), ortho- and para- H_2 , which differ in nuclear spin arrangement. This is because the equilibration is only slowly accomplished without the catalyst by changing temperature, and the triple-point temperature of H_2 depends on the composition of these isomers [2–4].

However, it has been recently confirmed that there is a problem for the triple point of e- H_2 when a large amount of powder of $\text{FeO}(\text{OH})$ is used as the catalyst; a large anomalous increase exists in the heat capacity at temperatures just below the triple point [2,5–8], and the anomalies markedly influence the shape of the melting plateau and the triple-point temperature [5–10]. Furthermore, a very recent report showed an anomalous double peak in the heat capacity just below the triple point using a sealed cell containing 89.7 mmol of H_2 with 0.53 g of powder of $\text{FeO}(\text{OH})$ [8]. The reduction of the amount of $\text{FeO}(\text{OH})$ suppresses the anomalies and makes the double-peak behavior unclear [8]. Clarification of the detailed behavior of the anomalies in the heat capacity has been expected to give a clue to understand its origin and one of the best ways to realize the triple-point temperature of e- H_2 at highest-level accuracy.

In this study, the heat capacity of e- H_2 with powder of $\text{FeO}(\text{OH})$ used as the catalyst was examined at temperatures around the triple point using sealed cells fabricated at the National Institute of Standards and Technology (NIST) and at the National Metrology Institute of Japan (NMIJ). Although these institutes used different sources of H_2 and $\text{FeO}(\text{OH})$ and different designs of sealed cells, the anomalous double peak has been evidently observed at both institutes in their heat capacities at temperatures just below the triple point.

We also tried to check the detailed behavior of the double peak in the heat capacity using NMIJ cells, and confirmed that the double peak occurs in the heat capacity independent of the amount of $\text{FeO}(\text{OH})$. Supercooling behavior characteristic of a first order phase transition also appears not only at the triple point but also at each anomalous peak, implying that the anomalous peaks could be caused by two or three coexisting parts within the solid H_2 . The part of the solid in close physical proximity to the catalyst appears to have a lower melting temperature due to an interaction between the powder of $\text{FeO}(\text{OH})$ and that portion of solid H_2 .

2. MEASUREMENTS

The designs of sealed cells fabricated at NIST and NMIJ are shown in Fig. 1a and b, respectively. The NIST cell consists of a stainless steel

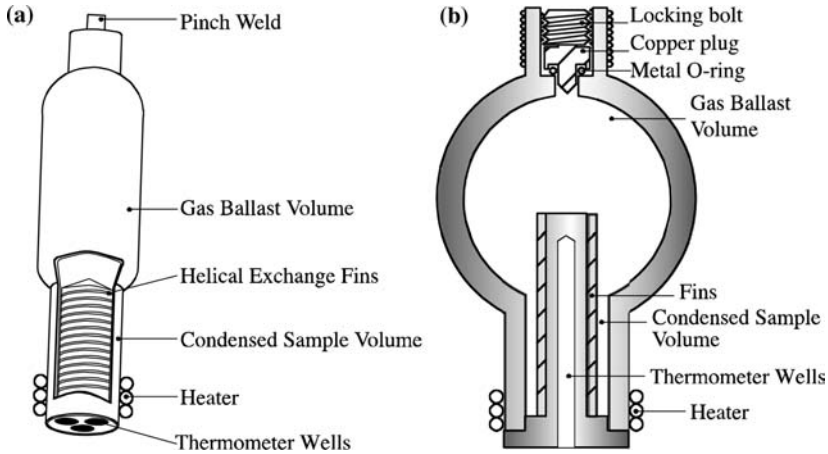


Fig. 1. Sealed cells: (a) fabricated at NIST [11] and (b) fabricated at NMIJ [8].

cylinder and copper insert with three thermometer wells. On the other hand, the NMIJ cell consists of only copper and its insert has one thermometer well. The inside of each sealed cell consists of a gas ballast volume, V_b , which is primarily for ballast in pressure, and a condensed sample volume, V_c , in which liquid and/or solid sample is condensed at low temperature. The volumes, V_b and V_c for NIST are about 40 and 3 cm^3 , respectively. On the other hand, the volumes, V_b and V_c for NMIJ are about 35 and 2 cm^3 , respectively. The detailed designs of these cells including gas filling systems and related techniques have been described elsewhere [8,9,11,12].

In this study, we used two NIST cells and three NMIJ cells. The NIST cells, 212 and 213, use H_2 obtained from MG Industries⁵, USA. The NMIJ cells, H-1, H-2, and H-5, use H_2 gas from Nippon Sanso⁵, Japan. The nominal chemical purity by volume of H_2 of all sources for both institutes is better than 99.9999%. A summary of the various cells contents, including isotopic composition of the gas, is given in Table I.

Measurements of the heat capacity around the triple point for $e\text{-H}_2$ sealed cells fabricated at NIST and at NMIJ have been carried out with the adiabatic calorimeters developed at the respective institutes. These

⁵ Certain commercial materials are identified in this paper to foster understanding. Such identification does not imply recommendation or endorsement by NIST and NMIJ/AIST, nor does it imply that the materials identified are necessarily the best available for the purpose.

Table I. Sealed-Cell Gas and Catalyst Content Summary

Cell ID	Institute	H ₂ (mmol)	m_{Cat}^a (g)	Catalyst Mesh	D/H ^b ($\mu\text{mol/mol}$)
H-1	NMIJ	85.5	0.53	<200	27.2
H-2	NMIJ	89.7	0.12	<200	27.2
H-5	NMIJ	89.7	0.015	<200	27.2
212	NIST	68	0.20	30–50	29.1
213	NIST	59	0.17	30–50	29.1

^a Mass of catalyst.

^b Deuterium content in hydrogen.

apparatus used at NIST and NMIJ and the detailed measurement procedures have been reported elsewhere. [8,9,11,12].

3. RESULTS AND DISCUSSION

3.1. Double Anomalous Peak in Heat Capacity of e-H₂ with Powder of FeO(OH)

Figure 2a and b show the heat capacities of e-H₂ cells fabricated at NIST (213) and at NMIJ (H-1, H-2, and H-5) near the triple point, respectively. An anomalous double extra peak, other than a divergence due to the triple point, is evidently observed for these cells at temperatures just below the triple point. Hereafter, each peak is referred to as an anomaly. The first anomaly, which is nearer to the triple point, is much larger than the second one. The anomalies in the NMIJ cells are very close in temperature to those in the NIST cell. Both anomalies are suppressed in magnitude by reducing the amount of the catalyst, as seen in Fig. 2b.

In the former report [8], the existence of second anomalies for cells H-2 and H-5 was unclear. But, the second anomaly can be clearly observed, even for cell H-5 including only 0.015 g of FeO(OH) by reducing the size of each heat pulse down to 0.005 J in the present study, as seen in the inset of Fig. 2b. Recently, Fellmuth et al. [13] also confirmed the anomalous double peak in the heat capacity of e-H₂ using some of the same sealed cells. These results indicate that the double peak-behavior in the heat capacity of e-H₂ with powder of FeO(OH) is a universal property independent of H₂ sources, FeO(OH) sources, and sealed-cell designs. Our results also show the position of the double peak is fairly insensitive to the amount of catalyst.

To investigate the dependence of the anomalies on the amount of FeO(OH), we focused on the data of NMIJ cells (H-1, H-2, and H-5)

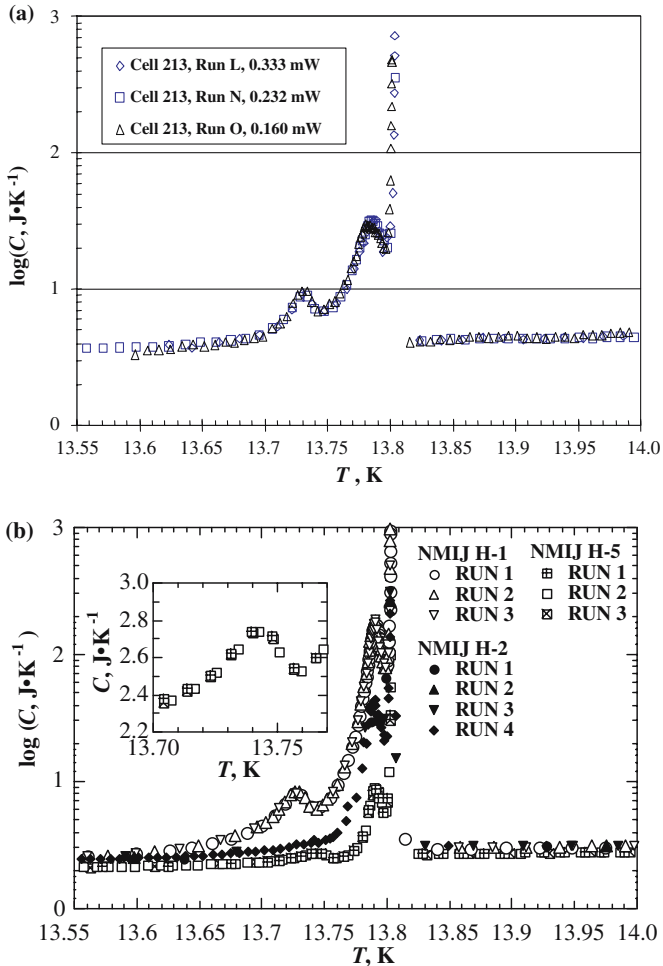


Fig. 2. Heat capacities near the triple point observed by using: (a) NIST cell 213 at three different heating powers and (b) H-1, H-2, and H-5 cells fabricated at NMIJ. The inset is an enlarged figure of the heat capacity of H-5 near the second anomaly.

including the same sources of H_2 and $\text{FeO}(\text{OH})$ and almost the same amount of H_2 . Figure 3 shows the enthalpy gain due to the anomalies and the triple-point transition of cell H-1 obtained from integration of the excess of heat capacity over the normal heat capacity in the same way reported in Ref. 8. The inset of Fig. 3 shows the dependence on the amount of $\text{FeO}(\text{OH})$ of the enthalpy gain due to the triple-point transition

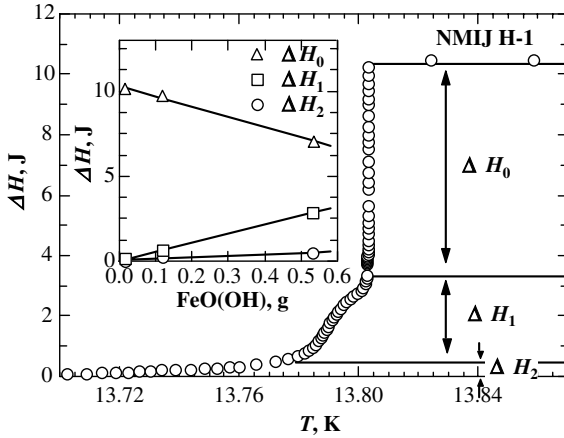


Fig. 3. Enthalpy gain due to the anomalies and the triple-point transition of cell H-1 obtained from integration of the excess of heat capacity over the normal heat capacity. The inset shows the dependence on the amount of catalyst of the enthalpy gains due to the triple-point transition (ΔH_0), first anomaly (ΔH_1), and second anomaly (ΔH_2).

(ΔH_0), first anomaly (ΔH_1), and second anomaly (ΔH_2). The sizes of ΔH_1 and ΔH_2 increase in proportion to the amount of the catalyst. This correlation strongly indicates that the catalyst causes both heat capacity anomalies, as reported previously [2, 5–9].

The total enthalpy gain due to both of the anomalies and the triple-point transition, $\Delta H_0 + \Delta H_1 + \Delta H_2$, is about 10 J and is consistent with the total heat of fusion expected from the amount of H_2 in each cell, as reported in Ref. 8. We also confirmed this agreement not only for cells H-1, H-2, and H-5 but also for cell 213. This strongly suggests that the anomalous double peak is related to the melting of a portion of the solid H_2 , as reported previously [8].

3.2. Heat Capacity of e- H_2 with Powder of FeO(OH) in its Supercooling State

Figure 4 shows the freezing curve of H_2 observed using cell H-1. The cooling power was about 20 mW. First, the temperature decreases to about 30 mK below the triple-point temperature because of supercooling. Next, the temperature jumps up to the triple-point temperature and stabilizes for about 9 hours because of solidification of H_2 at the triple point. Later, the temperature starts to decrease and shows a “shoulder” behavior around

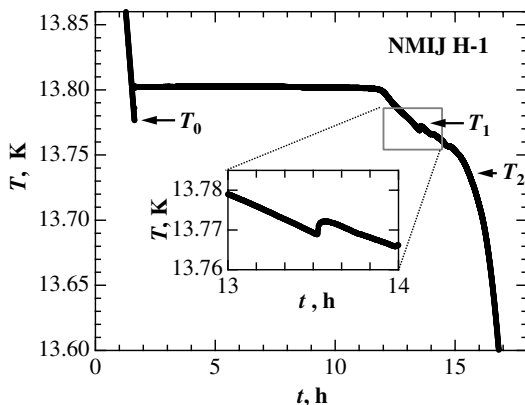


Fig. 4. Freezing curve observed by using cell H-1. The inset is an enlarged figure of the freezing curve near the shoulder behavior.

temperatures where the anomalies in the heat capacity have been observed. As seen in the inset of Fig. 4, there is a small peak in temperature around the shoulder. Finally, the temperature decreases steeply.

To check the heat capacity in the supercooling state, adiabatic calorimetry was started around the temperature T_0 in Fig. 4. To investigate the origin of the shoulder behavior, we also stopped the cooling at temperatures around the shoulder, T_1 and T_2 in Fig. 4, and then started measurements of heat capacity for cell H-1.

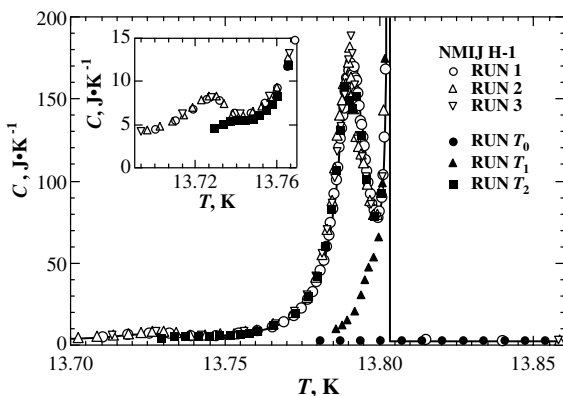


Fig. 5. Heat capacity of cell H-1, measurements that were started at temperatures T_0 , T_1 , and T_2 in Fig. 4.

Figure 5 shows the heat capacity of cell H-1, measurements of which were started at temperatures T_0 , T_1 , and T_2 in Fig. 4. The heat capacity of run T_0 , namely the heat capacity in the supercooled state, shows almost a constant behavior around the triple point without any anomaly at those temperatures, where the first anomaly was observed. This means that the anomalies will not occur without solid H_2 . It is consistent with the above suggestion that the anomalies are related to the melting of a portion of the solid H_2 .

As seen in Fig. 5, the heat capacity of run T_1 increases with increasing temperature without showing the first anomaly and agrees with the divergent part of the heat capacity due to the triple point at higher temperatures. This strongly suggests that the supercooling of the first anomaly phase will occur independently of the normal transition at the triple point. Similar behavior was also observed in run T_2 at temperatures around the second anomaly, as seen in the inset of Fig. 5. These results imply that the solid H_2 is segregated into three coexisting parts with three different melting temperatures. The shoulder behavior in Fig. 4 will be caused by the solidification of parts of H_2 with lower melting (freezing) temperatures.

Figure 6 shows a schematic view of solid H_2 with $FeO(OH)$ filled in a cell. The presence of the catalyst particles naturally segregates the solid H_2 into two volumes within the cell; one volume contains the solid H_2 coexisting with the catalyst $FeO(OH)$, and the other volume contains the solid H_2 separated from the catalyst. As mentioned above, the size of anomalies in the heat capacity shows a linear dependence on the amount of the catalyst [8,9]. So, the anomalies will come from the solid H_2 coexisting with the catalyst.

The catalysts being used for these sealed cells are prepared by precipitation from hydrous gels [14]. This process creates a very high porosity and hence a high active surface area when the gel is dried into the powder. An additional vacuum activation process is carried out either within

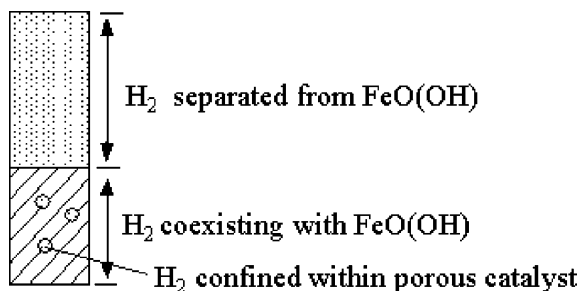


Fig. 6. Schematic view of solid H_2 with $FeO(OH)$ filled in a cell.

the cells prior to filling with H_2 or in a separate vacuum-reactor mainly to remove any remaining adsorbed H_2O and N_2 from these active surfaces. The condition of the catalyst activation procedure is as follows: 400 K for a day under vacuum at NIST, and 450 K for a week under vacuum at NMIJ [8,13,15]. Actually, a porous structure in powder of $\text{FeO}(\text{OH})$ is observed by using a scanning electron microscope [15]. The order of magnitude of diameter of pores is 100 nm. The detailed structure of pore will be shown elsewhere [15]. Probably, a part of H_2 confined within such a pore of catalyst (Fig. 6) will be followed by a depression of the melting temperature. It is possible that differences in the activation procedures used at NMIJ and NIST resulted in slight differences in the final chemical form and/or porosity of these catalysts, including the possibility of some catalyst transforming to anhydrous Fe_2O_3 .

Similar phenomena have been actually observed for H_2 in porous Vycor glass [16,17]. A shoulder behavior was observed in the freezing curve of H_2 in the Vycor pores below the triple-point temperature separate from a normal freezing plateau due to the solidification of H_2 outside of the Vycor pores [17]. It was also reported that a large peak appears on the heat capacity curves of H_2 in porous Vycor glass below the normal triple-point temperature of H_2 because of the depression of the melting temperature of H_2 in restricted geometries [16]. Furthermore, a double anomalous peak was observed resulting from the existence of two distinct pore radii in the pore-size distribution of Vycor glass [17]. As mentioned above, the anomalous double peak is observed in the heat capacity of $e\text{-H}_2$ with powder of $\text{FeO}(\text{OH})$. The reason for the appearance of the double peak is not clear from this study alone, but it may come from the existence of two distinct pore radii in the porous catalyst. Or it may be possible that the second (lower temperature) anomaly is caused by a solid-solid transition for that portion of the H_2 within the pores of the catalyst particles.

3.3. Melting Curves of $e\text{-H}_2$ at the Triple Point

The melting curves for H-1, H-2, and H-5 cells are shown in Fig. 7. The data obtained in heat capacity measurements are plotted against the inverse of the melted fraction, $1/F$. To evaluate F , ΔH_0 was used as the total heat of fusion. In Fig. 7, the melting curves reported in Ref. 8 are also shown. In Ref. 8, the melted fraction F was evaluated by using $\Delta H_0 + \Delta H_1 + \Delta H_2$ as the total heat of fusion; that is, the melting curves reported in Ref. 8 included the contribution of a portion of solid H_2 with lower melting temperatures due to the influence of the catalyst.

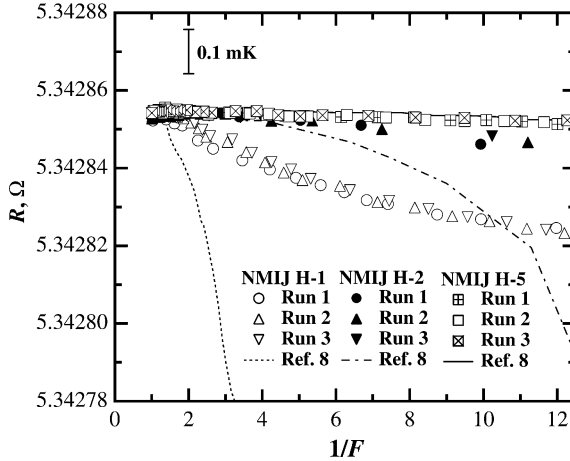


Fig. 7. Melting curves obtained by using cells H-1, H-2, and H-5. Dashed, dashed-dotted, and solid lines are melting curves reported in Ref. 8 for cells H-1, H-2, and H-5, respectively.

As seen in Fig. 7, the widths of the melting curves of cells H-1 and H-2 become narrow within about 0.2 mK in the wide region of $1/F$ up to $1/F=12$ by removing the contribution of ΔH_1 and ΔH_2 . On the other hand, both melting curves for H-5 obtained in the present study and in Ref. 8 show the same linear dependence on $1/F$. This is because the contributions of ΔH_1 and ΔH_2 for cell H-5 are very small as a result of the reduction of the amount of the catalyst.

The melting curves of cells H-1 and H-2 show almost the same value as cell H-5 at $1/F < 2$, but they deviate downward from the linear dependence of cell H-5 with increasing $1/F$ for $1/F > 2$ even though the contributions of ΔH_1 and ΔH_2 were removed. Probably, this suggests that the influence of the catalyst causing the suppression of the melting temperature will reach outside of the catalyst when a large amount of the catalyst was used.

Figure 8 shows melting curves of cells 212 and 213. The melted fraction F was evaluated by using $\Delta H_0 + \Delta H_1 + \Delta H_2$ as the total heat of fusion. Since both cells include the same ratio of the amounts of H_2 and $FeO(OH)$, the same behavior of the melting curves is expected. However, suppression of the melting temperature due to the catalyst is larger for cell 213 than that for cell 212 at higher $1/F$ values, as shown in Fig. 8.

If a correlation length of the influence of the catalyst exists outside of the catalyst as suggested above, the effect will depend on the amount of H_2 even if the same ratio of the amounts of H_2 and $FeO(OH)$ is included

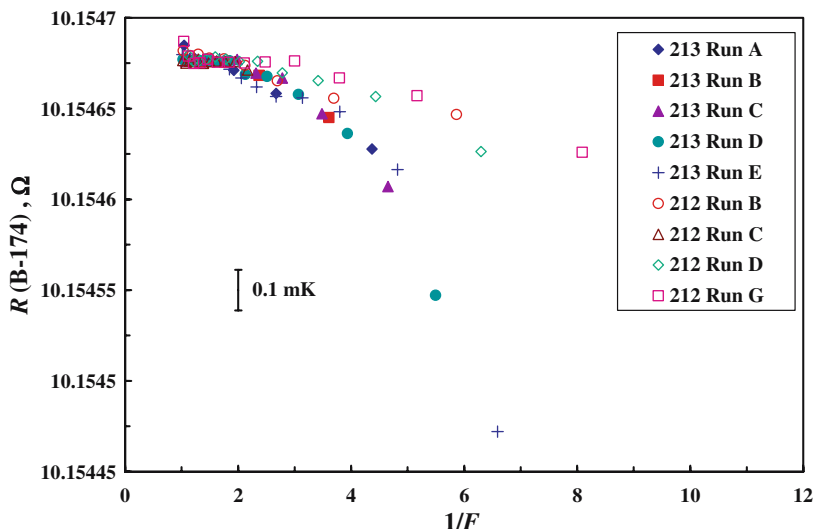


Fig. 8. Melting curves obtained by using NIST cells 212 and 213 under repeated melting runs.

in each cell; the influence of the catalyst will become larger for the case of the cell including a smaller amount of H_2 . This is consistent with the measurement result; the influence on the melting curve for cell 213 containing 59 mmol of H_2 is larger than that for cell 212 containing 68 mmol H_2 .

4. CONCLUSION

The heat capacity of $e\text{-H}_2$ with powder of $\text{FeO}(\text{OH})$ used as the catalyst for ortho-para-equilibration has been examined using sealed cells fabricated at the National Institute of Standards and Technology (NIST) and at the National Metrology Institute of Japan (NMIJ). An anomalous double peak appears in their heat capacities at temperatures just below the triple point independent of H_2 sources, $\text{FeO}(\text{OH})$ sources, and the designs of the sealed cells. The position of the double peak is fairly insensitive to the amount of catalyst. The supercooling behavior has been observed not only at the triple point but also at each anomalous peak, implying that the anomalous double peak will be caused by the depression of the melting temperature in restricted geometries or other endothermic transformations of the solid H_2 due to interactions between the catalyst and H_2 . A reduction of the amount of catalyst suppresses the influence of the catalyst and allows one to obtain more reliable melting curves for $e\text{-H}_2$.

ACKNOWLEDGMENT

The authors thank Dr. Shimazaki for his valuable discussions and useful suggestions.

REFERENCES

1. H. Preston-Thomas, *Metrologia* **27**:3 (1990), *ibid.*: 107 (erratum).
2. H. Sakurai, *T. SICE* **34**:1153 (1998).
3. *Supplementary Information for the International Temperature Scale of 1990*, BIPM (1990).
4. F. Pavese and G. Molinar, *Modern Gas-Based Temperature and Pressure Measurements* (Plenum Press, New York, 1992), Sub-section 2. 3. 2. 3.
5. H. Sakurai, in *Proc. TEMPMEKO 2001*, B. Fellmuth, J. Siedel, and G. Scholz, eds. (VDE Verlag GmbH, Berlin, 2002), pp. 411–416.
6. H. Sakurai, in *Temperature, Its Measurement and Control in Science and Industry*, Vol. 7, D. C. Ripple, ed. (American Institute of Physics, Melville, New York, 2003), pp. 969–974.
7. B. Fellmuth, D. Head, F. Pavese, A. Szmyrka-Grzebyk, and W. Tew, in *Proc. TEMPMEKO 2001*, B. Fellmuth, J. Siedel, and G. Scholz, eds. (VDE Verlag GmbH, Berlin, 2002), pp. 403–405.
8. T. Nakano, O. Tamura, and H. Sakurai, in *Temperature, Its Measurement and Control in Science and Industry*, Vol. 7, D. C. Ripple, ed. (American Institute of Physics, Melville, New York, 2003), pp. 185–190.
9. T. Nakano, O. Tamura, and H. Sakurai, *T. SICE* **38**:947 (2002).
10. A. G. Steele, in *Proc. TEMPMEKO 2001*, B. Fellmuth, J. Siedel, and G. Scholz, eds. (VDE Verlag GmbH, Berlin, 2002), pp. 417–422.
11. W. L. Tew, in *Proc. TEMPMEKO '96*, P. Marcarino, ed. (Levrotto and Bella, Torino, 1997), pp. 81–86.
12. C. W. Meyer and W. L. Tew, in *Temperature, Its Measurement and Control in Science and Industry*, Vol. 7, D. C. Ripple, ed. (American Institute of Physics, Melville, New York, 2003), pp. 137–142.
13. B. Fellmuth, L. Wolber, Y. Hermier, F. Pavese, P. P. M. Steur, I. Peroni, A. Szmyrka-Grzebyk, L. Lipinski, W. L. Tew, T. Nakano, H. Sakurai, O. Tamura, D. Head, K. D. Hill, and A. G. Steele, submitted to *Metrologia*.
14. P. L. Barrick, L. F. Brown, H. L. Hutchinson, and R. L. Cruse, *Adv. Cryo. Eng.* **10A**:181 (1965).
15. T. Nakano, O. Tamura, and H. Sakurai, submitted to *Proc. TEMPMEKO 2004*, June 22–25, 2004, Croatia.
16. J. L. Tell and H. J. Maris, *Phys. Rev. B* **28**:5122 (1983).
17. R. H. Torii, H. J. Maris, and G. M. Seidel, *Phys. Rev. B* **41**:7167 (1990).